Structural Engineering and Mechanics, *Vol. 67, No. 1 (2018) 9-20*
DOI: https://doi.org/10.12989/sem.2018.67.1.009

Dynamic analysis of high-speed railway train-bridge system after barge collision

Chaoyi Xia[1a], Qin Ma[2], Fudong Song[1b], Xuan Wu[1c] and He Xia*[1]

[1]School of Civil Engineering, Beijing Jiaotong University, Beijing 100044, China
[2]CCCC Highway Consultants Co., Ltd, Beijing 100088, China

(Received November 16, 2017, Revised April 11, 2018, Accepted April 13, 2018)

Abstract. In this paper, a framework is proposed for dynamic analysis of train-bridge systems with a damaged pier after barge collision. In simulating the barge-pier collision, the concrete pier is considered to be nonlinear-inelastic, and the barge-bow is modeled as elastic-plastic. The changes of dynamic properties and deformation of the damaged pier, and the additional unevenness of the track induced by the change of deck profile, are analyzed. The dynamic analysis model for train-bridge coupling system with a damaged pier is established. Based on the framework, an illustrative case study is carried out with a 5×32 m simply-supported PC box-girder bridge and the ICE3 high-speed train, to investigate the dynamic response of the bridge with a damaged pier after barge collision and its influence on the running safety of high-speed train. The results show that after collision by the barge, the vibration properties of the pier and the deck profile of bridge are changed, forming an additional unevenness of the track, by which the dynamic responses of the bridge and the car-body accelerations of the train are increased, and the running safety of high-speed train is affected.

Keywords: high-speed railway; concrete pier; barge collision; train-bridge system; dynamic response; running safety

1. Introduction

With the rapid development of HSR (high-speed railway) networks, many cross-river bridges have been constructed. In China, bridges play an important role in HSR. For example, the proportion of bridge length on the Beijing-Shanghai HSR line is more than 80%. While bridge piers located within waterways are necessary for supporting superstructure components, they constitute a potential obstacle to waterway vessel traffic. In the recent decades, the collapse accidents of bridges due to vessel collision were serious. According to the statistics by Dong *et al.* (2009) based on 502 collapse accidents of bridges in 66 countries, there were 91 collapse events caused by various collisions (by vessels 56, trucks and trains 33, and ice-floes 2), constituting 18% of the total bridge collapses, only preceded by earthquakes. A similar investigation by Wardhana and Hadipriono (2003) on 503 bridge collapses in the United States from 1989 to 2000 indicated that the most frequent causes of bridge failures were attributed to floods and collisions. Collisions from trucks, barge/ships, trains and others were responsible for 11.73% of the total bridge failures.

When a collision load acts on a bridge pier or a girder, it may cause damage on the pier or even unseating of bearings and girders, threatening the safety of bridge structure and the normal operation of train. For cross-river railway bridges, a recent example is the severe accident occurred in 2016 in China, when a sand barge collided to a pier of the Xiangtan Bridge on the Shanghai-Kunming railway line, as shown in Fig. 1. Due to this accident, the bridge pier was seriously damaged, and more than 20 trains through this bridge were delayed, leading to the bridge closed over 70 hours for repair.

Fig. 1 The barge collision accident happened on the Xiangtan Bridge (Huang 2016)

In the past years, researchers proposed various methods to solve the problem of ship-pier collision. For long-span bridges, different anti-collision facilities, such as anti-collision boxes, cofferdams and piles, have been used, and their applicability has been proved in theories and practices (Svensson 2009). However, for short-span bridges normally without special anti-collision facilities, the collisions may be serious when the piers are collided by a ship or barge running in a narrow navigation channel.

In the early studies, the primary method was to simplify the complex collision history as equivalent static collision

*Corresponding author, Professor
E-mail: hxia88@163.com
[a]Associate professor
[b]Graduate student
[c]Professor

ISSN: 1225-4568 (Print), 1598-6217 (Online)

loads, which were applicable in the anti-collision design of bridges by ship or barge as well as by vehicle, ice floe or other floating objects. Minorsky (1953) and Woisin (1976) proposed the empirical formula to calculate the ship collision load based on their tests. For barge collision, Meir-Dornberg (1983) conducted several pendulum hammer impact tests on the reduced-scale European hopper barges, and discussed the relation between the impact energy and the barge deformation. His research made a contribution to the Guide Specification and Commentary for Vessel Collision Design of Highway Bridges in the AASHTO (American Association of State Highway and Transportation Officials) code (1991). The AASHTO provisions make use of a series of empirical formulations relating kinetic energy to crush depth, and then crush depth to static force, which can be used to calculate the barge collision load. Nowadays, the anti-collision bridge design codes in most countries are based on the equivalent static loads.

With the development of numerical computation techniques, the whole history of collision can be simulated by FE (Finite Element) method. In most previous studies of this problem, the piers were assumed to be rigid or elastic. Yuan *et al.* (2008) conducted theoretical FE analysis on various types of flotilla impacting bridge piers, and proposed the design formulae for barge/flotilla impact loads. Using the LS-DYNA, Sha and Hao (2014) developed an accurate numerical model of barge-pier collision considering the plastic deformation and damage of the pier, and presented the impact force time histories with respect to various collision conditions. Fan *et al.* (2014) established a high-resolution FE model for ship-structure-soil interaction, and discussed the influences of material model, artificial boundary and stress initialization. Husem *et al.* (2016) analyzed the effect of support conditions on the displacements, energy absorption capacities and damage patterns of reinforcement concrete plates under impact loading by ABAQUS software. Walters *et al.* (2017) developed the Nonlinear dynamic FE models for barge flotillas, studied the inelastic barge crushing and the inter-barge wire-rope lashing behaviors over a wide range of conditions, and validated the numerical simulation results by the experimental data.

The dynamic analysis in the time-domain can predict the collision forces of structures accurately, and design-oriented time-history analysis techniques have been developed and validated (Consolazio *et al.* 2005, 2008). However, its wide use is limited due to the difficulty in establishing the FE model and the large computational effort. Therefore, researchers began to search other methods. Getter *et al.* (2011) proposed the equivalent static analysis method for barge impact-resistant design of bridges. Similar with the earthquake load, they proposed the response-spectrum analysis (RSA) procedure capable of directly predicting the maximum responses. Cowan *et al.* (2015) developed an RSA procedure for barge impact analysis of bridges, without yielding voluminous amounts of time-varying results, which is capable of directly producing maximum response parameters that are most pertinent to structural design. Fan *et al.* (2016) developed a specialized and reasonable combination rule for the shock-spectrum analysis (SSA) method, carried out a parametric study and explored the modal response characteristics of bridge structure subjected to barge impact.

For HSR bridges, the vessel collision may not only lead to a serious damage of the pier structure, but also deform the track on the bridge deck and make it instable, becoming a threat to the running safety of high-speed trains on the bridge. Laigaard *et al.* (1996) pointed out the problem of ship-induced derailment on a normal railway bridge, and evaluated the structural response subjected to a vessel collision by FE method. In China, Xuan and Zhang (2001) discussed the dynamic response of the bridge subjected to ship collision, and predicted its influence on the derailment of train on the bridge. Meanwhile, many researches have been done on the coupling vibrations of train-bridge system, and various analysis models were established to calculate the dynamic responses of tracks, bridge superstructures and substructures, as well as the running properties of trains (Frýba 2004, Xia *et al.* 2012, Rezvani *et al.* 2013, Jahangiri and Zakeri 2017, Podworna 2017). Among these researches, there have been several focused on the train-bridge system subjected to collision load, such as in the authors' previous works (Xia *et al.* 2014, 2016), where they did some researches towards the train-bridge system subjected to ship, vehicle and floating floes. In the published researches, most of the train-bridge system models were in elastic, while nonlinear behaviors such as plastic hinge formation were considered for piers struck by barges (Davidson *et al.* 2013). Yin *et al.* (2016) simulated the crack zone in the reinforced concrete bridge by a damage function and investigated the vibration behaviors of a damaged bridge under moving vehicles. However up to now, few if any studies have analyzed post-collision dynamic performance of the bridge during train passages while taking into account damage to piers.

When the collision of barge on the pier is intense, the plastic deformation at pier top may change the deck profile of the bridge, forming an additional unevenness on the track irregularity, which may change the smoothness of the track, and influence the dynamic behaviors of the train-bridge system. Therefore, it is necessary to use the plastic pier model and consider the deck profile change of the bridge induced by the plastic displacement at pier top in the analysis model to evaluate the operation function of the damaged structure and the running behaviors of high-speed train. To this end, this paper presents a framework for performing dynamic analysis on the train-bridge system with damaged pier induced by barge collision. The barge colliding on the bridge pier is simulated by FE method, in which the pier is considered to be nonlinear-inelastic, and the barge-bow is elastic-plastic. After calculation, the changes of dynamic properties and deformation of the damaged pier, as well as the additional unevenness of the track induced by the change of deck profile, are obtained. The dynamic analysis model for train-bridge coupling system with damaged pier is established. Then, the dynamic responses of an ICE3 high-speed train running through a 5×32 m simply-supported PC box-girder bridge with damaged pier are analyzed, and the running properties of the train are evaluated.

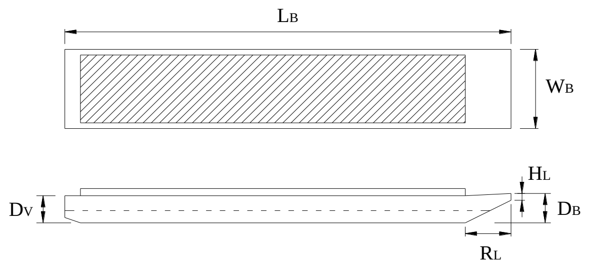

Fig. 2 Plane and elevation views of the hopper barge in AASHTO Code

Table 1 Dimensions of the hopper barge

Item	Dimension
L_B (Full length)	195 ft (59.4 m)
W_B (Full width)	35 ft (10.7 m)
D_V (Full depth)	12 ft (3.7 m)
D_B (Depth of Bow)	13 ft (4.0 m)
R_L (Length of Bow Rake)	20 ft (6.1 m)
H_L (Height of Head Log)	3 ft (0.91 m)

2. Analysis model for barge-pier collision

The analysis model for barge-pier collision is established by using the software of LS-DYNA (LS-DYNA User Manual 2007). The model consists of two parts: the barge model and the simplified pier model.

2.1 Barge model

The Jumbo hopper barge (hopper barge for short hereinafter) obtained from the AASHTO (1991), which has been used in barge-pier collision analysis by many researchers, is chosen as the barge model in the collision simulation. In this analysis, the barge with total weight of 1900t is adopted. The plane and elevation views of the hopper barge are shown in Fig. 2, and the specific dimensions of the barge are listed in Table 1.

In the barge model, the rib beams of the barge hull framing structure are established with the Beam161 elements in LS-DYNA, and the steel plates with the thickness of 0.013 m supported by the framing structure are established with the Shell163 elements. To reduce the computational effort, the steel material for the barge-bow elements is set to be in elastic-plastic state, while those for the other elements of the barge are in elastic. The elastic-plastic behaviour of structural steel of the barge-bow is described by the Cowper-Symonds equation

$$\frac{\sigma_d}{\sigma_s} = 1 + \left(\frac{\dot{\varepsilon}}{C}\right)^{1/P} \tag{1}$$

where, σ_d is the dynamic yield stress, σ_s is the static yield stress, $\dot{\varepsilon}$ is the effective strain rate; C and P are parameters for material strain rate, and they are set to be 40.5 and 5, respectively. Moreover, the mechanical performance of the structural steel is achieved by using the "MAT_PLASTIC_ KINEMATIC" model in LS-DYNA.

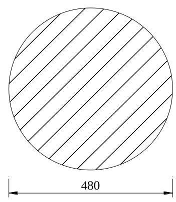

(a) Cross-section of round pier (unit: cm)

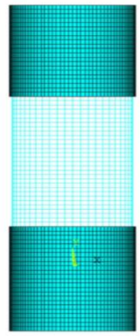

(b) Arrangement of reinforcement bars

Fig. 3 Cross-section and reinforcement arrangement of bridge pier

2.2 Pier model

There are various types of piers used in HSR bridges in China, with different section forms, such as the hollow rectangular section, solid round section, and solid round-ended section. For the bridge across navigation channel, the solid piers with round and round-ended section are more suitable for resisting the river streams. The difference is that the round pier is more often used for the river with unfixed flow direction, while the round-ended one is for the river of fixed flow direction. In this paper, the round pier used to support the 32 m simply-supported PC box-girders in HSR bridges is chosen for analysis. Shown in Fig. 3(a) are the cross-section and arrangement of reinforcement bars of the pier.

Normally, the amount of reinforcement bars in a pier is represented by reinforcement ratio φ, which is defined as the ratio of the total area of longitudinal steel bars to the whole area of the pier cross-section. In the Code for Design of High-speed Railways (TB10621 2014) in China, there is no special regulation toward the reinforcement ratio for bridge piers, but in actual design, there is a trend to use low reinforcement percentage, where the reinforcement percentage smaller than 0.5 is usually preferred (Chen *et al.* 2016). To study the possible influence of barge collision on the dynamic response of piers with such low reinforcement percentage, two kinds of reinforcement ratios, φ=0.2% and φ=0.4%, are selected for the bridge pier. For φ=0.2%, the longitudinal steel reinforcements with a diameter of 30 mm are arranged with 300 mm spacing, and the lateral reinforcements with diameter of 20 mm are arranged with 200 mm spacing along the pier height, as shown in Fig. 3(b). For φ=0.4%, the longitudinal steel reinforcements with a diameter of 30 mm are arranged with 150 mm spacing, and the lateral reinforcements are arranged the same as whose for φ=0.2%. The reinforcement steel bars

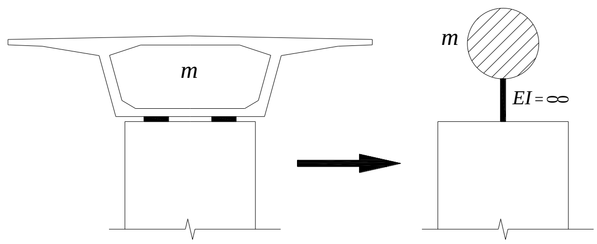

Fig. 4 Analysis model of the bridge pier

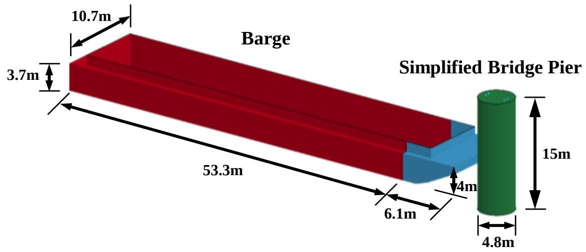

Fig. 5 The FE model of barge colliding on bridge pier

Table 2 Material property parameters of the concrete pier

Concrete parameter	Elastic	Nonlinear
Density (kg/m^3)	2340	2340
Young's modulus (MPa)	2.28×10^4	2.28×10^4
Poisson's ratio	0.2	0.2
Failure strain	--	0.1
Unconfined compressive strength (MPa)	--	40

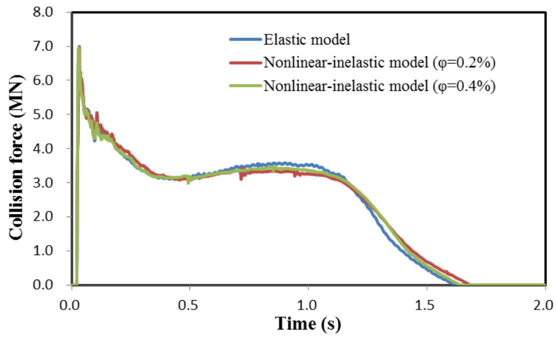

Fig. 6 Time histories of collision loads of a barge on round pier

are established by using the Beam161 Element in LS-DYNA. The Elements of solid concrete pier and reinforcement steel bars are coupled together by merging nodes at same positions. The reinforcements in the FE model are simulated by using the "MAT_PIECEWISE _LINEAR_PLASTICITY" model in LS-DYNA.

Shown in Fig. 4 is the analysis model of the bridge pier. In the model, the Solid164 elements in LSDYNA are adopted to simulate the pier, and the foundation of the pier is supposed to be fixed on the ground. To simplify the calculation, the girders on the pier are not directly modelled with finite elements, but their masses are simulated by the Mass144 element on the pier-top, with its mass equals to that of the 32 m simply-supported PC box-girder. The Solid elements and the Mass element are connected almost rigidly, by setting a high value for the bending inertia moment of the connection element.

The mechanical properties of concrete material subjected to collision load are very complicated. Tu and Lu (2009) evaluated several typical material models for dynamic properties of concrete subjected to impact loads, and proved that the Concrete Damage Model in LS-DYNA is valid. Then, a new version model named "Concrete Damage Release III" is issued in LS-DYNA, which is simpler for collision simulation (LS-DYNA User Manual 2007). The principle of this new concrete model has been studied by many scholars (Malvar *et al.* 1994, Markovich *et al.* 2011). The model provides a capability of generating the parameters automatically, which makes an easier use of the concrete damage model, thus no special material test is necessary. Therefore, the "Concrete Damage Release III" model is adopted in this paper to consider the nonlinear behaviour and to simulate the damage of the concrete.

By inputting the density, Poisson's ratio and unconfined compressive strength of the concrete material in Table 2, the 49 parameters, which are required to define an equation of state (EOS), damage function, failure surfaces and constitutive behaviour of the concrete material under different confinement pressures, are automatically generated by the LS-DYNA software.

3. Collision force of HSR bridge pier under a barge collision

According to the AASHTO, the average navigation velocity of the hopper barge is 2.06 m/s (4 knots), thus the running velocity of the barge is firstly set to be 2.0 m/s in the analysis. The height of the bridge pier is 15 m, and the cross-section of the pier is round with the diameter of 4.8 m. The FE model for this case study is shown in Fig. 5.

The whole histories of the hopper barge colliding on the simplified pier model are simulated by the LS-DYNA. To obtain the time history of the collision load and to increase the calculation efficiency, the mass scaling switch is open in the analysis. The material of the concrete pier is assumed to be in two cases, elastic and nonlinear-inelastic, respectively, and the time histories of the collision loads are shown in Fig. 6.

From the figure, it can be observed that the time histories of collision forces for both the elastic and nonlinear-inelastic piers exhibit two phases: the drastic "sharp" loading curves with a short duration for 0.2-0.3 s at the beginning phase, and the relatively "flat" loading curves with a longer duration for 1.2-1.3 s at the followed phase. The beginning phase and the followed phase are also called as initial phase and remaining phase, respectively (Larson, 1993). The peak force on the elastic pier is 6.94 MN, which is almost equal to 7.00 MN and 6.96 MN on the nonlinear-inelastic pier with φ=0.2% and φ=0.4%, respectively. Although the time histories of collision loads in Fig. 6 are similar, it is still important to consider the nonlinear properties of bridge pier in calculation, as evidenced in the following sections, where the pier's damage induced by

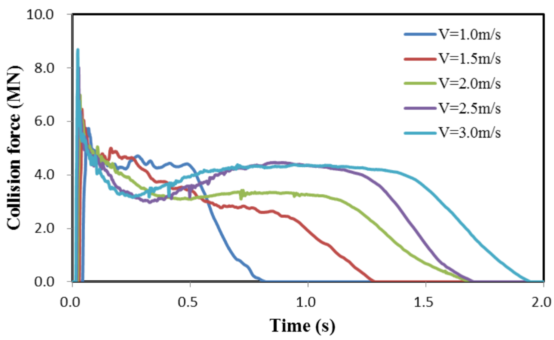

(a) φ=0.2%

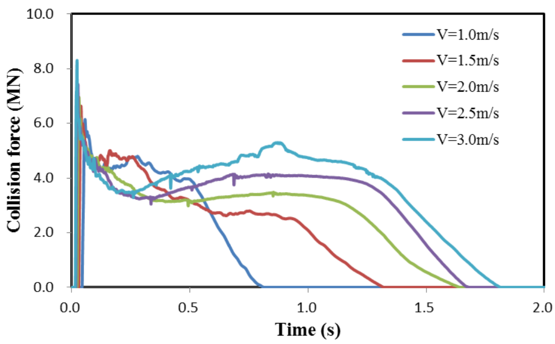

(b) φ=0.4%

Fig. 7 Time histories of collision loads under various barge velocities

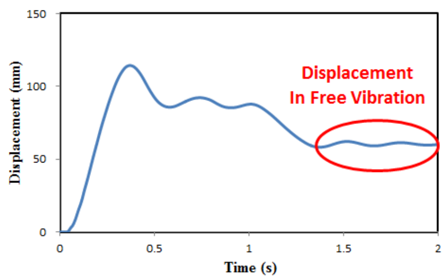

(a) Time history domain

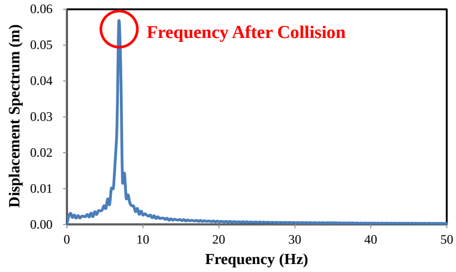

(b) Frequency domain

Fig. 8 Lateral displacement at pier-top after barge collision

collision is examined and the running safety of train passaging on the bridge is checked. However, it is difficult to estimate the damage effect of bridge pier only by observing the peak values and time history curves of barge collision, and this topic will be discussed in the following analysis.

In the *Fundamental Code for Design on Railway Bridge and Culvert in China* (TB10002.1 2005), the design vessel collision load is expressed as

$$F = \gamma v \sin\alpha \sqrt{\frac{W}{C_1 + C_2}} \tag{2}$$

where: F is the collision load (kN); γ is the reduction coefficient of kinetic energy (s/m$^{1/2}$), which is 0.3 for the barge colliding on the pier in forward direction, and 0.2 for slanting direction; v is the navigation velocity of the barge (m/s); α is the colliding angle of barge with the pier; W is the total weight of the barge (kN); C_1 and C_2 are elastic parameters respectively for the barge and the bridge pier (m/kN), and C_1+C_2 can be taken as 0.0005 m/kN when lack of material information.

For the barge with navigation velocity of 2.0 m/s, the design collision load by Eq. (5) is 3.66 MN, which is much smaller than the simulated maximum collision load 7.00 and 6.96 MN in the nonlinear-inelastic piers with different reinforcement ratios and 6.94 MN in the elastic pier. It seems that the collision load in design is insufficient to avoid the collision induced failure. In fact, the design load in the code is generally based on the elastic theory, which cannot reflect the damage of bridge pier when heavier, faster and more complicated vessel collision is applied, therefore, nonlinear-inelastic response of the pier should be considered, which will be discussed in the following sections.

In reality, the collision loads may be different for vessels with various velocities. In the AASHTO code, the maximum vessel velocity concerned is 3.09 m/s (6 knots), so in the next analysis, the collision forces on the pier are calculated by considering the vessel velocity from 1.0 m/s to 3.0 m/s. Shown in Fig. 7 are the calculated time histories of collision loads induced by the elastic-plastic barge-bow at different barge velocities.

From the calculation results, the influence of barge velocity on the collision force properties can be observed. When the barge velocity is lower than 2.0 m/s, the time history curves of the collision load exhibit a similar characteristic like elastic collision, and their durations at the remaining phase are short. With the increase of barge velocity, the peak values are enlarged and the remaining phase durations are elongated, while the initial phase durations are shortened. Generally, the faster the barge velocity, the higher the peak values and the longer the durations of collision loads. Compared with the collision on the elastic pier, the average collision forces on the nonlinear-inelastic pier at the remaining phase are much smaller, which also shows the property of nonlinear-inelastic material of bridge pier.

4. Dynamic characteristics of HSR bridge pier after barge collision

Owing to the high requirement on the running safety of high-speed trains, the damage of HSR bridge pier induced by barge collision should be concerned. In practice, the dynamic properties such as natural frequencies are often used to evaluate the structural safety. Because the vibration induced by barge collision is in lateral direction, and the

Table 3 The 1st lateral frequencies of the pier after collision

Barge velocity (m/s)	Elastic material (Hz)	Nonlinear-inelastic model (Hz)		Allowance value in Code (Hz)
		φ=0.2%	φ=0.4%	
1.0		4.639	6.592	
1.5		3.418	5.859	
2.0	8.849	3.845	6.470	3.106
2.5		4.089	6.347	
3.0		4.150	7.268	

Table 4 Residual deformations at the top of pier after collision

Barge velocity (m/s)	Elastic material (m)	Nonlinear-inelastic model (m)		Allowance value in Code (m)
		φ=0.2%	φ=0.4%	
1.0		0.0431	0.0200	
1.5		0.0604	0.0254	
2.0	--	0.0486	0.0228	--
2.5		0.0376	0.0201	
3.0		0.0319	0.0189	

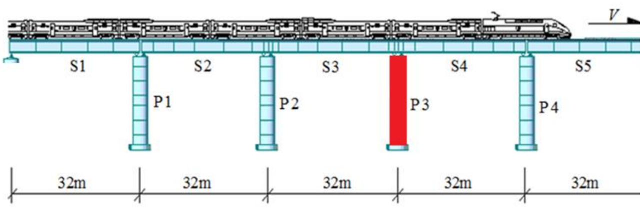

(a) Plane view

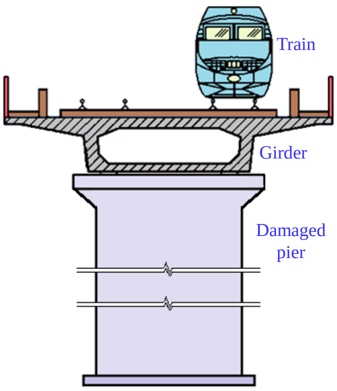

(b) Sectional view

Fig. 9 Train-bridge coupling system with a damaged pier after barge collision

running safety of high-speed train is mainly affected by the lateral structural vibration, the natural frequency related to the first lateral mode is essential for evaluating the safety of pier structure.

In this case, the pier with round section suffers a collision by the barge with velocity of 2.0 m/s. The time history of the displacement at pier-top is extracted, as shown in Fig. 8(a).

From Fig. 8(a), it can be seen that the time history curve of displacement contains several stages: at the beginning of collision, the displacement increases and reaches to the peak value rapidly; after that, it keeps steady during the destruction of barge bow; then it decreases with the barge leaving the bridge pier due to the rebound effect. Because the material is set to be inelastic, the displacement cannot return to the original position, and pier is in free vibration around the residual deformation induced by barge collision.

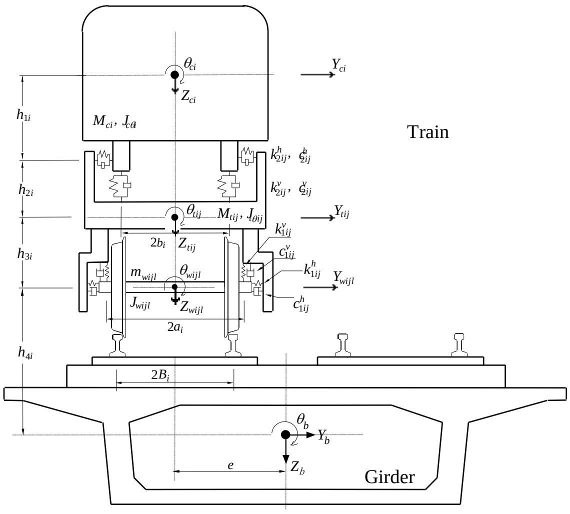

Fig. 10 Dynamic model of Train-bridge system

By using the Fast Fourier Transform, the displacement at pier-top can be transformed into frequency domain, and its spectrum distribution is shown in Fig. 8(b). From the figure, the 1st frequency after collision can be obtained. Listed in Table 3 are the 1st frequencies of the round piers, and in Table 4 are the related residual deformations at pier-top after barge collision.

By comparison, it can be found that the frequencies for the first lateral modes of the pier are obviously reduced after it is collided by a barge. Normally, it is believed that the damage would be more serious when the bridge suffers a collision with faster barge, but the results show a different phenomenon that the frequencies and plastic deformation at pier-top do not change monotonically with the increase of barge velocity. This phenomenon is quite similar with the conclusions in reference (Sha and Hao 2012), which also indicates that increasing the impact velocity does not always result in a larger pier displacement.

5. Running safety analysis of high-speed train on bridge after barge collision

In this section, the running safety of the high-speed train running on the bridge with a damaged pier after barge collision is analyzed. The bridge is composed of 5×32 m simply-supported PC box girders with double tracks, as shown in Figs. 9 and 10.

In the analysis, the pier P3 in the navigation channel is supposed to be damaged due to the barge collision and the plastic displacement is generated at the pier-top, and the other piers are in healthy.

By modal analysis, the natural frequencies and mode shapes of the first 10 modes of the bridge can be obtained, as listed in Table 5.

Table 5 Natural frequencies and mode descriptions of the first 10 modes of the bridge

Healthy bridge			Bridge with damaged pier			
			φ=0.2%		φ=0.4%	
Descriptions of mode shapes	Mode No.	Frequency (Hz)	Mode No.	Frequency (Hz)	Mode No.	Frequency (Hz)
Lateral symmetric bending of the whole bridge	1	3.438	1	2.713	1	3.154
Lateral antisymmetric bending of the whole bridge	2	3.908	2	3.802	2	3.842
Vertical antisymmetric bending of the 1st and 5th spans	3	3.943	3	3.912	3	3.927
Vertical symmetric bending of the whole bridge	4	4.099	4	4.073	4	4.091
Vertical antisymmetric bending of the 2nd and 4th spans	5	4.114	5	4.111	5	4.112
Vertical symmetric bending of the whole bridge	6	4.126	6	4.126	6	4.126
Vertical symmetric bending of the 1st and 5th spans	7	4.586	8	4.584	8	4.585
Lateral symmetric bending of the whole bridge	8	4.635	7	4.469	7	4.549
Lateral antisymmetric bending of the whole bridge	9	5.509	9	5.165	9	5.297
Vertical antisymmetric bending of the 1st and 5th spans	10	8.213	10	8.110	10	8.160

From the table above, it can be seen that the natural frequencies of bridge with damaged pier decrease clearly comparing with the healthy bridge. With the reduction of reinforcement ratio, the natural frequencies especially the lateral frequencies of the bridge decline remarkably, which shows that the effect of barge collision on pier is mainly in lateral direction and the influence of reinforcement ratio is obvious.

5.1 Description of analysis model

The dynamic analysis model of train-bridge system with a damaged pier is established. In the system model, the train subsystem model is established by the rigid-bodies with elastic connections, and the bridge subsystem model is established by the finite element method. The two subsystems are coupled by the wheel-rail interaction, and the combined unevenness of the track is regarded as the internal excitation of the two subsystems. When the bridge subsystem model is established by the modal decomposition method, the coupled motion equations for the train-bridge dynamic system after the pier is damaged after the barge-pier collision can be expressed as

$$\begin{bmatrix} \mathbf{M}_{\mathrm{vv}} & 0 \\ 0 & \mathbf{M}_{\mathrm{bb}} \end{bmatrix}\begin{Bmatrix} \ddot{\mathbf{X}}_{\mathrm{v}} \\ \ddot{\mathbf{Q}}_{\mathrm{b}} \end{Bmatrix}+\begin{bmatrix} \mathbf{C}_{\mathrm{vv}} & \tilde{\mathbf{C}}_{\mathrm{vb}} \\ \tilde{\mathbf{C}}_{\mathrm{bv}} & \tilde{\mathbf{C}}_{\mathrm{bb}} \end{bmatrix}\begin{Bmatrix} \dot{\mathbf{X}}_{\mathrm{v}} \\ \dot{\mathbf{Q}}_{\mathrm{b}} \end{Bmatrix} +\begin{bmatrix} \mathbf{K}_{\mathrm{vv}} & \tilde{\mathbf{K}}_{\mathrm{vb}} \\ \tilde{\mathbf{K}}_{\mathrm{bv}} & \tilde{\mathbf{K}}_{\mathrm{bb}} \end{bmatrix}\begin{Bmatrix} \mathbf{X}_{\mathrm{v}} \\ \mathbf{Q}_{\mathrm{b}} \end{Bmatrix}=\begin{Bmatrix} \tilde{\mathbf{F}}_{\mathrm{vb}} \\ \tilde{\mathbf{F}}_{\mathrm{bv}} \end{Bmatrix} \tag{3}$$

where: the subscript "v" and "b" represent train vehicle and bridge, respectively; the superscript "~" denotes that the matrix is related to the bridge with damaged pier after the barge collision; $\mathbf{X}_{\mathrm{v}}$, $\dot{\mathbf{X}}_{\mathrm{v}}$ and $\ddot{\mathbf{X}}_{\mathrm{v}}$ are the displacement, velocity and acceleration vectors of the train subsystem, respectively; $\mathbf{Q}_{\mathrm{b}}$, $\dot{\mathbf{Q}}_{\mathrm{b}}$ and $\ddot{\mathbf{Q}}_{\mathrm{b}}$ are the displacement, velocity and acceleration vectors of the modal coordinate of the bridge, expressed as

$$\mathbf{Q}_{\mathrm{b}}=\begin{bmatrix} q_1 & q_2 & \cdots & q_n & \cdots & q_{N_{\mathrm{b}}} \end{bmatrix}=\tilde{\mathbf{\Phi}}^{\mathrm{T}}\mathbf{X}_{\mathrm{b}} \tag{4}$$

where: q_n is the nth modal coordinate of the bridge; $\tilde{\mathbf{\Phi}}$ is the mode-shape matrix of the bridge after the barge-pier collision; N_{b} is the total number of the bridge modes concerned.

M_{vv}, C_{vv} and K_{vv} are the mass, damping and stiffness matrices of the train subsystem itself, which are not changed after the barge-pier collision, thus details of them are the same as those in the common train-bridge system, and can be found in the authors' previous works (Xia *et al.* 2012, 2014, 2016).

The submatrices of $\tilde{\mathbf{M}}_{\mathrm{bb}}$, $\tilde{\mathbf{C}}_{\mathrm{bb}}$ and $\tilde{\mathbf{K}}_{\mathrm{bb}}$ are the mass, damping and stiffness matrices of the bridge subsystem after the barge-pier collision, respectively expressed as

$$\tilde{\mathbf{M}}_{\mathrm{bb}}=\begin{bmatrix} 1+M_{\mathrm{b}}^{11} & M_{\mathrm{b}}^{12} & \cdots & M_{\mathrm{b}}^{1N_{\mathrm{b}}} \\ M_{\mathrm{b}}^{21} & 1+M_{\mathrm{b}}^{22} & \cdots & M_{\mathrm{b}}^{2N_{\mathrm{b}}} \\ \cdots & \cdots & \ddots & \cdots \\ M_{\mathrm{b}}^{N_{\mathrm{b}}1} & M_{\mathrm{b}}^{N_{\mathrm{b}}2} & \cdots & 1+M_{\mathrm{b}}^{N_{\mathrm{b}}N_{\mathrm{b}}} \end{bmatrix} \tag{5}$$

in which

$$M_{\mathrm{b}}^{nm}=\sum_{i=1}^{N_{\mathrm{v}}}\sum_{j=1}^{2}\sum_{l=1}^{N_{\mathrm{w}i}}(\tilde{\Phi}_{\mathrm{h}ijl}^{nm}\cdot m_{\mathrm{w}ijl}+\tilde{\phi}_{\theta ijl}^{nm}\cdot J_{\mathrm{w}ijl}+\tilde{\Phi}_{\mathrm{v}ijl}^{nm}\cdot m_{\mathrm{w}ijl})$$

(i=1,2,…, N_v; n=1,2,…, N_b; j=1,2);

$$\tilde{\mathbf{K}}_{\mathrm{bb}}=\begin{bmatrix} \tilde{\omega}_1^2+K_{\mathrm{b}}^{11} & K_{\mathrm{b}}^{12} & \cdots & K_{\mathrm{b}}^{1N_{\mathrm{b}}} \\ K_{\mathrm{b}}^{21} & \tilde{\omega}_2^2+K_{\mathrm{b}}^{22} & \cdots & K_{\mathrm{b}}^{2N_{\mathrm{b}}} \\ \cdots & \cdots & \ddots & \cdots \\ K_{\mathrm{b}}^{N_{\mathrm{b}}1} & K_{\mathrm{b}}^{N_{\mathrm{b}}2} & \cdots & \tilde{\omega}_{N_{\mathrm{b}}}^2+K_{\mathrm{b}}^{N_{\mathrm{b}}N_{\mathrm{b}}} \end{bmatrix} \tag{6}$$

in which

$$K_{\mathrm{b}}^{nm}=\sum_{i=1}^{N_{\mathrm{v}}}\sum_{j=1}^{2}\sum_{l=1}^{N_{\mathrm{w}i}}(\tilde{\Phi}_{\mathrm{h}ijl}^{nm}\cdot k_{1ij}^{\mathrm{h}}+\tilde{\phi}_{\theta ijl}^{nm}\cdot k_{1ij}^{\mathrm{v}}a_i^2+\tilde{\Phi}_{\mathrm{v}ijl}^{nm}\cdot k_{1ij}^{\mathrm{v}})$$

(i=1,2,…, N_v; n=1,2,…, N_b; j=1,2);

$$\tilde{\mathbf{C}}_{\mathrm{bb}}=\begin{bmatrix} 2\xi\tilde{\omega}_1+C_{\mathrm{b}}^{11} & C_{\mathrm{b}}^{12} & \cdots & C_{\mathrm{b}}^{1N_{\mathrm{b}}} \\ C_{\mathrm{b}}^{21} & 2\xi\tilde{\omega}_2+C_{\mathrm{b}}^{22} & \cdots & C_{\mathrm{b}}^{2N_{\mathrm{b}}} \\ \cdots & \cdots & \ddots & \cdots \\ C_{\mathrm{b}}^{N_{\mathrm{b}}1} & C_{\mathrm{b}}^{N_{\mathrm{b}}2} & \cdots & 2\xi\tilde{\omega}_{N_{\mathrm{b}}}+C_{\mathrm{b}}^{N_{\mathrm{b}}N_{\mathrm{b}}} \end{bmatrix} \tag{7}$$

in which

$$C_{\mathrm{b}}^{nm}=\sum_{i=1}^{N_{\mathrm{v}}}\sum_{j=1}^{2}\sum_{l=1}^{N_{\mathrm{w}i}}(\tilde{\Phi}_{\mathrm{h}ijl}^{nm}\cdot c_{1ij}^{\mathrm{h}}+\tilde{\phi}_{\theta ijl}^{nm}\cdot c_{1ij}^{\mathrm{v}}\cdot a_i^2+\tilde{\Phi}_{\mathrm{v}ijl}^{nm}\cdot c_{1ij}^{\mathrm{v}})$$

(i=1,2,…, N_v; n=1,2,…, N_b; j=1,2);

In the above matrices,

$\tilde{\Phi}^{nm}_{\mathrm{h}ijl} = (\tilde{\phi}^{n}_{\mathrm{h}ijl} + h_{4i}\cdot\tilde{\phi}^{n}_{\theta ijl})\cdot(\tilde{\phi}^{m}_{\mathrm{h}ijl} + h_{4i}\cdot\tilde{\phi}^{m}_{\theta ijl})$, $\tilde{\phi}^{nm}_{\theta ijl} = \tilde{\phi}^{n}_{\theta ijl}\cdot\tilde{\phi}^{m}_{\theta ijl}$, $\tilde{\Phi}^{nm}_{\mathrm{v}ijl} = (\tilde{\phi}^{n}_{\mathrm{v}ijl} + e_i\cdot\tilde{\phi}^{n}_{\theta ijl})\cdot(\tilde{\phi}^{m}_{\mathrm{v}ijl} + e_i\cdot\tilde{\phi}^{m}_{\theta ijl})$, and $\tilde{\phi}^{n}_{\mathrm{h}ijl}$, $\tilde{\phi}^{n}_{\mathrm{v}ijl}$ and $\tilde{\phi}^{n}_{\theta ijl}$ are the mode-shapes of the bridge deck at the rail position in lateral, vertical and rotational direction, respectively; N_v is the total amount of vehicles in the train, and $N_{\mathrm{w}i}$ is the number of wheel-sets on the jth bogie of the ith vehicle. $m_{\mathrm{w}ijl}$ and $J_{\mathrm{w}ijl}$ are the mass and mass moment of inertia of the lth wheel-set on the jth bogie of the ith vehicle of the train; k^{h}_{1ij} and k^{v}_{1ij} are the lateral and vertical stiffnesses of the primary suspension between the lth wheel-set and the jth bogie; $\tilde{\omega}_1, \tilde{\omega}_2, ...\tilde{\omega}_{N_\mathrm{b}}$ are the frequencies of the 1st, 2nd, …, N_bth mode related to the bridge with damaged pier after the barge-pier collision. From the analysis in Sec.4, it can be found that the vibration frequencies of the bridge are reduced and the profile of bridge deck is changed after the pier suffers a barge collision, thus the mode-shape and frequency vectors in the above equations should use those of the bridge after collision.

The submatrices $\tilde{\mathbf{K}}_{\mathrm{vb}}$ and $\tilde{\mathbf{K}}_{\mathrm{bv}}$ are the stiffness matrices between the train subsystem and the bridge subsystem after the barge-pier collision, respectively, expressed as

$$\tilde{\mathbf{K}}_{\mathrm{vb}} = \{\tilde{\mathbf{K}}_{\mathrm{bv}}\}^{\mathrm{T}} = \begin{bmatrix} \tilde{\mathbf{K}}_{\mathrm{v_1 b}} \\ \tilde{\mathbf{K}}_{\mathrm{v_2 b}} \\ \cdots \\ \tilde{\mathbf{K}}_{\mathrm{v}_{N_\mathrm{v}}\mathrm{b}} \end{bmatrix} \tag{8}$$

In $\tilde{\mathbf{K}}_{\mathrm{vb}}$, the submatrices $\tilde{\mathbf{K}}_{\mathrm{v_1 b}}$, $\tilde{\mathbf{K}}_{\mathrm{v_2 b}}$, …, $\tilde{\mathbf{K}}_{\mathrm{v}_{N_\mathrm{v}}\mathrm{b}}$ represent the influence matrices of bridge on the 1st, 2nd, …, N_vth vehicle of the train. The ith submatrix can be expressed as

$$\tilde{\mathbf{K}}_{\mathrm{v}_i\mathrm{b}} = \begin{bmatrix} \mathbf{0} & \mathbf{0} & \cdots & \mathbf{0} \\ \tilde{\mathbf{K}}^{i}_{\mathrm{t_1 q_1}} & \tilde{\mathbf{K}}^{i}_{\mathrm{t_1 q_2}} & \cdots & \tilde{\mathbf{K}}^{i}_{\mathrm{t_1 q}_{N_\mathrm{b}}} \\ \tilde{\mathbf{K}}^{i}_{\mathrm{t_2 q_1}} & \tilde{\mathbf{K}}^{i}_{\mathrm{t_2 q_2}} & \cdots & \tilde{\mathbf{K}}^{i}_{\mathrm{t_2 q}_{N_\mathrm{b}}} \end{bmatrix} \tag{9}$$

For the ith car, because it has two bogies t^i_1 and t^i_2, the submatrices $\tilde{\mathbf{K}}^{i}_{\mathrm{t}_j\mathrm{q}_1}, \tilde{\mathbf{K}}^{i}_{\mathrm{t}_j\mathrm{q}_2}, ..., \tilde{\mathbf{K}}^{i}_{\mathrm{t}_j\mathrm{q}_{N_\mathrm{b}}}$ are the influence stiffness matrices of the 1st, 2nd……N_bth modal coordinate of the bridge on the jth bogie of the ith car. The sub mactirx $\tilde{\mathrm{K}}^{i}_{\mathrm{t}_j\mathrm{q}_n}$ is

$$\tilde{\mathbf{K}}^{i}_{\mathrm{t}_j\mathrm{q}_n} = -\sum_{l=1}^{N_{\mathrm{w}i}} \begin{bmatrix} (\tilde{\phi}^{n}_{\mathrm{h}ijl} + h_{4i}\cdot\tilde{\phi}^{n}_{\theta ijl})\cdot k^{\mathrm{h}}_{1ij} \\ \tilde{\phi}^{n}_{\theta ijl}\cdot a_i^2\cdot k^{\mathrm{v}}_{1ij} - h_{3i}\cdot\tilde{\phi}^{n}_{\mathrm{h}ijl}\cdot k^{\mathrm{h}}_{1ij} \\ \eta_{jl}\cdot d_i\cdot\tilde{\phi}^{n}_{\mathrm{h}ijl}\cdot k^{\mathrm{h}}_{1ij} \\ (\tilde{\phi}^{n}_{\mathrm{v}ijl} + e_i\cdot\tilde{\phi}^{n}_{\theta ijl})\cdot k^{\mathrm{v}}_{1ij} \\ \eta_{jl}\cdot d_i\cdot\tilde{\phi}^{n}_{\mathrm{v}ijl}\cdot k^{\mathrm{v}}_{1ij} \end{bmatrix} \tag{10}$$

where, h_{3i} is the vertical distance between the centroids of bogie and wheel-set of the ith vehicle. a_i is the half lateral distance between the primary suspension of the ith car. d_i is the half longitudinal distance between the two wheel-sets on the same bogie. e_i is the half track pitch. η_{jl} is the position function of wheel-set, which equals to 1 for the front wheel-set on a bogie, and -1 for rear wheel-set on the same bogie.

The sub-damping matrices $\tilde{\mathbf{C}}_{\mathrm{vb}}$ and $\tilde{\mathbf{C}}_{\mathrm{bv}}$ are the damping matrices between the train subsystem and the bridge subsystem after the barge-pier collision, respectively, which can be obtained by simply replacing "k" in the corresponding sub-stiffness matrix by "c".

$\mathbf{F}_{\mathrm{vb}}$ and $\mathbf{F}_{\mathrm{bv}}$ are the inter-force vectors of the bridge structure and the train vehicles, respectively.

For the interaction force applied on the train,

$$\tilde{\mathbf{F}}_{\mathrm{vb}} = [\tilde{\mathbf{F}}_{\mathrm{v_1 b}} \quad \tilde{\mathbf{F}}_{\mathrm{v_2 b}} \quad \cdots \quad \tilde{\mathbf{F}}_{\mathrm{v}_{N_\mathrm{b}}\mathrm{b}}]^{\mathrm{T}} \tag{11}$$

where, $\tilde{\mathbf{F}}_{\mathrm{v}_i\mathrm{b}}$ is the inter-force vector acting on the ith vehicle of the train,

$$\tilde{\mathbf{F}}_{\mathrm{v}_i\mathrm{b}} = [\mathbf{0} \quad \tilde{\mathbf{F}}^{\mathrm{t_1}}_{\mathrm{v}_i\mathrm{b}} \quad \tilde{\mathbf{F}}^{\mathrm{t_2}}_{\mathrm{v}_i\mathrm{b}}]^{\mathrm{T}} \tag{12}$$

where $\tilde{\mathbf{F}}^{\mathrm{t_1}}_{\mathrm{v}_i\mathrm{b}}$ and $\tilde{\mathbf{F}}^{\mathrm{t_2}}_{\mathrm{v}_i\mathrm{b}}$ are the vectors of forces transmitted from the wheel-sets through the primary springs and dashpots to the front and rear bogies of the ith vhicle, respectively, and can be described as

$$\tilde{\mathbf{F}}^{\mathrm{t}_j}_{\mathrm{v}_i\mathrm{b}} = \sum_{l=1}^{N_{\mathrm{w}i}} \begin{Bmatrix} k^{\mathrm{h}}_{1ij}\cdot\tilde{Y}_{\mathrm{s}}(x_{ijl}) \\ a_i^2\cdot k^{\mathrm{v}}_{1ij}\cdot\tilde{\theta}_s(x_{ijl}) - h_{3i}\cdot k^{\mathrm{h}}_{1ij}\cdot\tilde{Y}_{\mathrm{s}}(x_{ijl}) \\ \eta_{jl}\cdot d_i\cdot k^{\mathrm{h}}_{1ij}\cdot\tilde{Y}_{\mathrm{s}}(x_{ijl}) \\ k^{v}_{1ij}\cdot\tilde{Z}_{\mathrm{s}}(x_{ijl}) \\ \eta_{jl}\cdot d_i\cdot k^{v}_{1ij}\cdot\tilde{Z}_{\mathrm{s}}(x_{ijl}) \end{Bmatrix} \tag{13}$$

$(i=1,2,\ldots, N_\mathrm{v};\quad j=1,2)$

where, $\tilde{Y}_{\mathrm{s}}(x_{ijl})$, $\tilde{Z}_{\mathrm{s}}(x_{ijl})$ and $\tilde{\theta}_s(x_{ijl})$ are the combined unevennesses of the track in lateral, vertical and rotational directions at the lth wheel-set on the jth bogie of the ith vehicle, and x_{ijl} is the travelling position of the wheel-set.

For the interaction force applied on the bridge,

$$\tilde{\mathbf{F}}_{\mathrm{bv}} = [F_{\mathrm{b_1 v}} \quad F_{\mathrm{b_2 v}} \quad \cdots \quad F_{\mathrm{b}_{N_\mathrm{b}}\mathrm{v}}]^{\mathrm{T}} \tag{14}$$

The force vector for the nth mode of bridge is

$$\begin{aligned} F_{\mathrm{b}_n\mathrm{v}} = \sum_{i=1}^{N_\mathrm{v}}\sum_{j=1}^{2}\sum_{l=1}^{N_{\mathrm{w}i}} \Big\{ & [(\tilde{\phi}^{n}_{\mathrm{h}ijl} + h_{4i}\cdot\tilde{\phi}^{n}_{\theta ijl})\cdot k^{\mathrm{h}}_{1ij}\cdot\tilde{Y}_{\mathrm{s}}(x_{ijl}) \\ & + \tilde{\phi}^{n}_{\theta ijl}\cdot k^{\mathrm{v}}_{1ij}\cdot a_i^2\cdot\tilde{\theta}_{\mathrm{s}}(x_{ijl}) + (\tilde{\phi}^{n}_{\mathrm{v}ijl} + e_i\cdot\tilde{\phi}^{n}_{\theta ijl})\cdot k^{v}_{1ij}\cdot\tilde{Z}_{\mathrm{s}}(x_{ijl})] \\ & + \tilde{\phi}^{n}_{\mathrm{v}ijl}\cdot g\cdot[m_{\mathrm{w}ijl} + (0.5M_{\mathrm{c}i} + M_{\mathrm{t}ij})/N_{\mathrm{w}i}]\Big\} \end{aligned} \tag{15}$$

where, M_{ci} is the mass of the ith car-body, and M_{tij} is the mass of the jth bogie of the ith car.

In the analysis, the combined unevennesses of the track are composed of the original track irregularities and the changed profile of bridge deck induced by the damaged pier after barge collision. The original track irregularity is

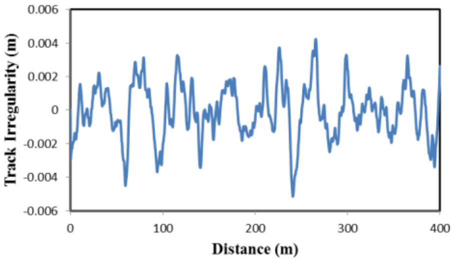

(a) Original track irregularity

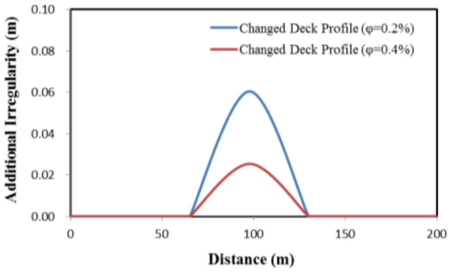

(b) Changed deck profile

Fig. 11 The combined track unevenness after collision

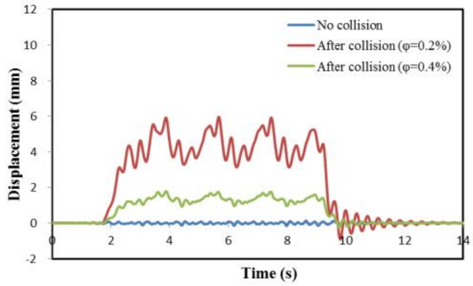

(a) At mid-spam of S4

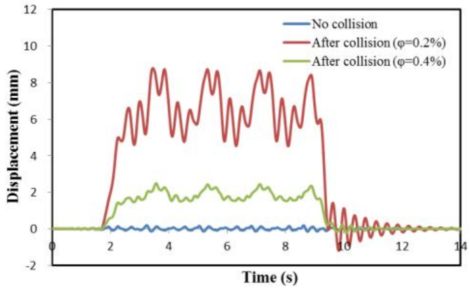

(b) At top of P3

Fig. 12 Lateral displacements of the bridge

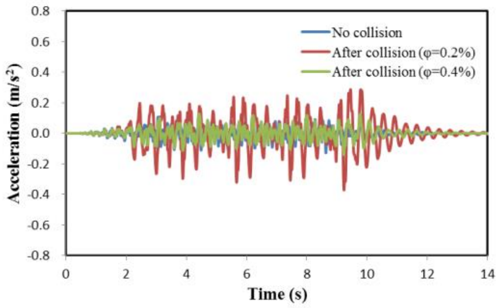

(a) At mid-span of S4

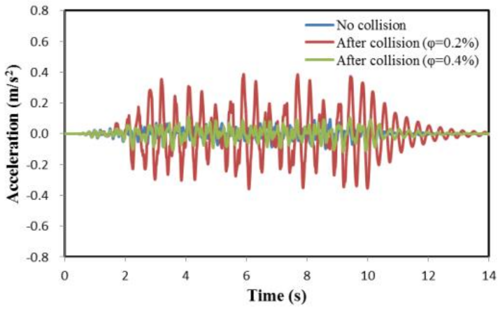

(b) At top of P3

Fig. 13 Lateral accelerations of the bridge

generated according to the Germany Low Disturbance Irregularity Spectrum, as shown in Fig. 11(a), and the changed profiles of bridge deck induced by the plastic deformations of the pier after the collision of the barge with V=1.5 m/s are shown in Fig. 11(b).

The train in this case study concerned is the ICE3 train composed of 4×(3M+1T), where M and T represent the motor-car and trailer-car respectively. The properties and dimensions of ICE3 train can be found in the authors' previous work (Xia *et al.* 2017). The round piers with diameter of 4.8 m are considered, as shown in Fig. 3. The train speeds in the calculation are 200, 220, 240, 260, 280, 300, 320 and 340 km/h.

In the analysis, the dynamic equations of the train-bridge system are solved using the Newmark implicit step-by-step integration algorithm with β = 1/4. A computer code is written based on the formulation derived above and is used to perform the calculation.

5.2 Calculation results

5.2.1 Dynamic response of bridge

When a pier is damaged after a barge collision, its lateral stiffness will decrease, which may influence the operation properties of the bridge. In Chinese railway, the dynamic displacements of girders and piers are used to evaluate the operation properties of bridge structure. According to the *Code for Rating Operational Performance of HSR Bridge in China* (TG/GW209 2014, hereinafter the Bridge Rating Code for short), the usual value of lateral mid-span displacement for 32 m girders is 0.15 mm, and the usual value of lateral pier-top displacement is

$$\Delta_{\text{usual}} = \frac{H_{\text{p}}}{60B} + 0.03 \tag{16}$$

where: Δ_{usual} is the usual value of lateral pier-top displacement (mm), which is equal to 0.082 mm in this case; B is the width of the pier in lateral direction (m); and H_{p} is the height of the pier (m). In the Bridge Rating Code, the usual values are based on the statistical analysis of measured values at the bridges on the current operation HSR lines.

Since the dynamic responses at the mid-spans of S3 and S4 connected with damaged pier are similar, herein only the time histories of lateral displacements at the mid-span of S4 and the top of P3 are presented, when the train passes through the bridge with the speed of 200 km/h, as shown in Fig. 12.

From the figures, it can be found that: (1) the lateral displacements of the bridge after collision are much greater than those without collision; (2) the lateral displacement at top of the damaged pier P3 is greater than those at mid-span of S4, which is connected with the damaged pier; (3) the maximum lateral displacements are 5.97 mm at the mid-span of S4 and 8.79 mm at the top of damaged pier P3, respectively, which far exceed the usual values given in the Bridge Rating Code.

Shown in Fig. 13 are the time histories of lateral accelerations of the bridge at the mid-spans of S4 and the top of P3 when the train passes through with the speed of 200 km/h.

It can be seen that: (1) the accelerations at top of P3 and at mid-spans of S4 after collision are much higher than those without collision; (2) the lateral acceleration at top of the damaged pier P3 is greater than those at mid-span of S4.

From Figs. 12 and 13 one can see that the displacements and accelerations of the bridge with the reinforcement ratio of φ = 0.2% are almost 4 times as those with φ = 0.4%, which indicates that the adopting reasonable reinforcement ratio is an effective measure to resist the barge collision.

5.2.2 Running safety of high-speed train

In high-speed railway system, the running safety of the train is highly concerned. The evaluation indices for the running safety of train currently adopted in high-speed railways in China include: the derailment factor Q/P_1 (defined as the ratio of the lateral wheel-rail force Q to the vertical force P_1 of the wheel at the climbing-up-rail side), the offload factor $\Delta P/\bar{P}$ (defined as the ratio of the offloaded vertical wheel-rail force DP to the average vertical wheel-rail force $\bar{P}$ of the two wheels on a wheel-set) and the lateral wheel-rail force Q. The expressions and allowable values of these indices given in *Railway Vehicle Specification for Evaluating the Dynamic Performance and Accreditation Test* (GB5599-85 1985) are as follows

$$\begin{aligned} &\text{Derailment factor:} && Q/P_1 \le 0.8 \\ &\text{Offload factor:} && \Delta P/\bar{P} \le 0.6 \\ &\text{Wheel/rail force:} && Q \le 0.85(10 + P_{st}/3) \end{aligned} \tag{17}$$

where, P_{st} denotes the static wheel-set load in kN. The allowable lateral wheel-rail forces for the motor-car and trailer-car of the ICE3 high-speed train are 52.97 kN and 49.08 kN, corresponding to their static loads of 156.96 kN and 143.23 kN, respectively.

In addition to the running safety of train, the comfortability is another important factor to evaluate the operational properties of train-bridge system. In this case study, the limit for lateral acceleration of car-body is used to evaluate the comfort degree of the train, which is 1.0 m/s^2 stipulated in the *Code for Design of High Speed Railway* (TB10621-2014 2014).

Because the collision load is in lateral direction, while the profile of bridge deck in vertical direction is small, the offload factor is not considered in the following analysis.

Fig. 14 shows the distributions of maximum derailment factors, lateral wheel-rail forces and lateral car-body accelerations of the high-speed train running through the bridge with damaged pier after barge collision.

From the figures, it can be found that:

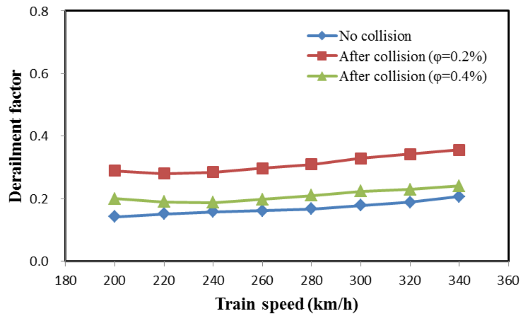

(a) Derailment factor

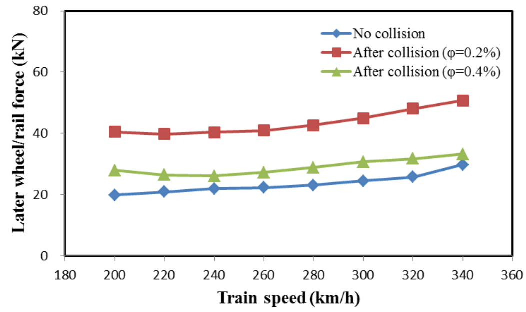

(b) Lateral wheel/rail force of motor car

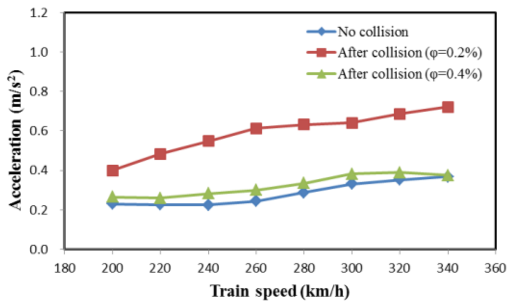

(c) Lateral acceleration of car-body

Fig. 14 Maximum running safety indices of the high-speed train

(1) In all cases, on the general trend, the derailment factors, lateral wheel-rail forces and lateral car-body accelerations increase with the train speed when the train passes the bridge at 200 km/h to 340 km/h.

(2) Before the barge collision on the pier, the maximum derailment factor, lateral wheel-rail force and lateral car-body acceleration are 0.207, 29.79 kN and 0.368 m/s^2, respectively, and all of the indices are lower than their related allowance values.

(3) After the pier is collided by the barge, for the pier with φ=0.2%, the maximum derailment factor, lateral wheel-rail force and lateral car-body acceleration are increased to 0.356, 50.70 kN and 0.721 m/s^2, which are 1.72, 1.70 and 1.96 times of those before the collision, respectively. It is noticed that the lateral wheel/rail force for φ=0.2% is very close to the allowance value of 52.97 kN.

(4) For the pier with φ=0.4%, as expected, the situation is improved: the maximum derailment factor, lateral wheel-rail force and lateral car-body acceleration are 0.241, 33.25 kN and 0.375 m/s^2, respectively. Compared with those for the pier with φ=0.2%, they are reduced by 32.3%, 34.4% and 48.0%, respectively.

6. Conclusions

In this paper, a framework for dynamic analysis of the train-bridge system with damaged pier after barge collision was proposed. The changes of the dynamic properties of the damaged pier and the additional unevenness of the track induced by the change of deck profile were analyzed. Based on the framework, an illustrative case study was carried out with a 5×32 m simply-supported PC box-girders bridge and the ICE3 EMU high-speed train, to investigate the dynamic response of the bridge with a damaged pier after barge collision and its influence on the running safety of high-speed train. The following conclusions can be drawn from the case study:

• For the collision force of barge on the pier, the peak values are enlarged and the remaining phase durations are elongated with the increase of barge velocity, while the initial phase durations are shortened. Generally, the faster the barge velocity, the greater the peak value and the longer the duration of collision load. Compared with the collision on the elastic pier, the average collision force on the nonlinear-inelastic pier at the remaining phase is much lower.

• After collided by the barge, the vibration frequencies of the pier are lowered, and the plastic deformation are generated at the pier-top, thus the deck profile of bridge is changed by the plastic deformation of the pier-top, forming an additional unevenness of the track.

• When the high-speed train runs on the bridge with the additional track unevenness induced by the changed deck profile, the vibration responses of bridge, as well as the running safety indices and car-body accelerations of the train are degraded. In the case study, the maximum lateral wheel/rail forces of trains become very close to the allowance value.

• The reinforcement ratio of pier has an important influence on the dynamic response of train-bridge system, especially for the bridge with nonlinear-inelastic pier. When the reinforcement ratio of pier is increased form φ=0.2% to φ=0.4%, the vibration frequencies of the pier is increased obviously and the plastic displacements at pier-top (as well as the additional unevenness of track induced by the change of deck profile) become much smaller, which result in smaller dynamic responses of the bridge and the high-speed train.

Acknowledgments

The study is supported by the Fundamental Research Funds for the Central Universities (2015RC006) of China.

References

AASHTO (1991), *Guide Specification and Commentary for Vessel Collision Design of Highway Bridges*, Volume I, Final Report, Washington, U.S.A.

Chen, X.C., Zhang, Y.L., Ding, M.B. and Li, X.Z. (2016), “Study of minimum reinforcement ratios for concrete piers arranged with small amount of reinforcement under rare earthquake”, *Bridg. Constr.*, **46**(5), 24-28.

Consolazio, G.R. and Michael, D. (2008), “Simplified dynamic analysis of barge collision for bridge design”, *J. Trans. Res. Board*, **2050**(2008), 13-25.

Consolazio, G.R. and Cowan, D.R. (2005), “Numerically efficient dynamic analysis of barge collisions with bridge piers”, *J. Struct. Eng.*, **131**(8), 1256-1266.

Cowan, D.R., Consolazio, G.R. and Davidson, M.T. (2015), “Response-spectrum analysis for barge impacts on bridge structures”, *ASCE J. Bridg. Eng.*, **20**(12), 04015017.

Davidson, M.T., Consolazio, G.R., Getter, D.J. and Shah, F.D. (2013), “Probability of collapse expression for bridges subject to barge collision”, *J. Bridg. Eng.*, **18**(4), 287-296.

Dong, Z.F., Guo, J. and Wang, J.J. (2009), “Review of bridge collapse and prevention measures”, *Highw.*, **16**(2), 30-32.

Fan, W. and Yuan, W.C. (2014), “Numerical simulation and analytical modeling of pile-supported structures subjected to ship collisions including soil-structure interaction”, *Ocean Eng.*, **91**, 11-27.

Fan, W., Zhang, Y.Y. and Liu, B. (2016), “Modal combination rule for shock spectrum analysis of bridge structures subjected to barge collisions”, *J. Eng. Mech.*, **142**(2), 04015083.

Frýba, L. (2004), “Dynamic behavior of bridges due to high speed trains”, *Proceedings of the Bridges for High Speed Railways*, Porto, Portugal.

GB5599-85 (1985), *Railway Vehicle Specification for Evaluating the Dynamic Performance and Accreditation Test*, National Bureau of Standards, Beijing, China.

Getter, D.J., Consolazio, G.R. and Davidson, M.T. (2011), “Equivalent static analysis method for barge impact-resistant bridge design”, *J. Bridg. Eng.*, **16**(6), 718-727.

Huang, H. (2016), “The Xiangtan railway bridge on Shanghai-Kunming railway line was collided by a ship and the trains passing the bridge were delayed”, *Xinmin Net*.

Husem, M. and Cosgun, S.I. (2016), “Behavior of reinforced concrete plates under impact loading: Different support conditions and sizes”, *Comput. Concrete*, **18**(3), 389-404.

Jahangiri, M. and Zakeri, J.A. (2017), “Dynamic analysis of train-bridge system under one-way and two-way high-speed train passing”, *Struct. Eng. Mech.*, **64**(1), 33-44.

Laigaard, J.J., Svensson, E. and Ennemark, E. (1996), “Ship-induced derailment on a railway bridge”, *Struct. Eng.*, **6**(2), 107-112.

Larson, O.D. (1993), *Ship Collision with Bridges*, Struct. Eng. Docum. No. 4, IABSE Switzerland.

LS-DYNA User Manual (2007), Version 971, Livermore Software Tech. Corp., Livermore, California, U.S.A.

Malvar, L.J., Crawford, J.E., Wesevich, J.W. and Simons, D. (1994), *A New Concrete Material Model for DYNA3D, Karagozian & Case*, Glendale, California, U.S.A.

Markovich, N., Kochavi, E. and Ben-Dor, G. (2011), “An improved calibration of the concrete damage model”, *Fin. Elem. Analy. Des.*, **47**(11), 1280-1290.

Meir-Dornberg, K.E. (1983), “Ship collisions, safety zones, and loading assumptions for structures in inland waterways”, *VDI Berichte*, **496**(1), 1-9.

Minorsky, N. (1953), “On interaction of non-linear oscillations”, *J. Frankl. Inst.*, **256**(2), 147-165.

Mosayebi, S.A., Zakeri, J.A. and Esmaeili, M. (2017), “Vehicle/track dynamic interaction considering developed railway substructure models”, *Struct. Eng. Mech.*, **61**(6), 775-784.

Podworna, M. (2017), “Dynamic response of steel-concrete composite bridges loaded by high-speed train”, *Struct. Eng. Mech.*, **62**(2), 179-196.

Rezvani, M.A., Vesali, F. and Eghbali, A. (2013), “Dynamic response of railway bridges traversed simultaneously by

opposing moving trains", *Struct. Eng. Mech.*, **36**(5), 713-734.
Sha, Y.Y. and Hao, H. (2012), "Nonlinear finite element analysis of barge collision with a single bridge pier", *Eng. Struct.*, **41**, 63-76.
Svensson, H. (2009), "Protection of bridge piers against ship collision", *Steel Constr.*, **2**(1), 21-35.
TB10002.1 (2005), *Fundamental Code for Design on Railway Bridge and Culvert in China*, China Railway Publishing House, Beijing, China.
TB10621-2014 (2015), *Code for Design of High Speed Railway*, China Railway Publishing House, Beijing, China.
TG/GW209 (2014), *Code for Rating Operational Performance of HSR Bridge in China*, China Railway Publishing House, Beijing, China.
Tu, Z. and Lu, Y. (2009), "Evaluation of typical concrete material models used in hysdrocodes for high dynamic response simulations", *Int. J. Imp. Eng.*, **36**(1), 132-146.
Walters, R.A., Davidson, M.T., Consolazio, G.R. and Patev, R.C. (2017), "Characterization of multi-barge flotilla impact forces on wall structures", *Mar. Struct.*, **51**, 21-39.
Wardhana, K. and Hadipriono, F.C. (2003), "Analysis of recent bridge failures in the United States", *J. Perform. Constr. Facil.*, **17**(3), 144-150.
Woisin, G. (1976), "The collision tests of the GKSS", *Jahrbuch Schiffbautech Gesellsch*, **70**, 465-487.
Xia, H., De Roeck, G. and Goicolea, J.M. (2012), *Bridge Vibration and Controls: New Research*, Nova Science Publishers Inc., New York, U.S.A.
Xia, H., Zhang, N. and Guo, W.W. (2017), *Dynamic Interaction of Train-Bridge Systems in High-Speed Railways-Theory and Applications*, Springer Nature, Berlin, Germany.
Xia, C.Y., Xia, H. and De, R.G. (2014), "Dynamic response of a train–bridge system under collision loads and running safety evaluation of high-speed trains", *Comput. Struct.*, **140**(6), 23-38.
Xia, C.Y., Zhang, N., Xia, H., Ma, Q. and Wu, X. (2016), "A framework for carrying out train safety evaluation and vibration analysis of a trussed-arch bridge subjected to vessel collision", *Struct. Eng. Mech.*, **59**(4), 683-701.
Xuan, Y. and Zhang, D. (2001), "Derailment of train induced by vessel collision on railway bridge pier", *Bridg. Abroad*, **19**(4), 60-64.
Yin, X.F., Liu, Y. and Kong, B. (2016), "Vibration behaviors of a damaged bridge under moving vehicular loads", *Struct. Eng. Mech.*, **58**(2), 199-216.
Yuan, P., Harik, I.E. and Davidson, M.T. (2008), *Multi-Barge Flotilla Impact Forces on Bridges*, Research Report, Kentucky Transportation Center, University of Kentucky, U.S.A.

CC